Article

Cell Reports

Identification of Serotonergic Neuronal Modules that Affect Aggressive Behavior

Graphical Abstract

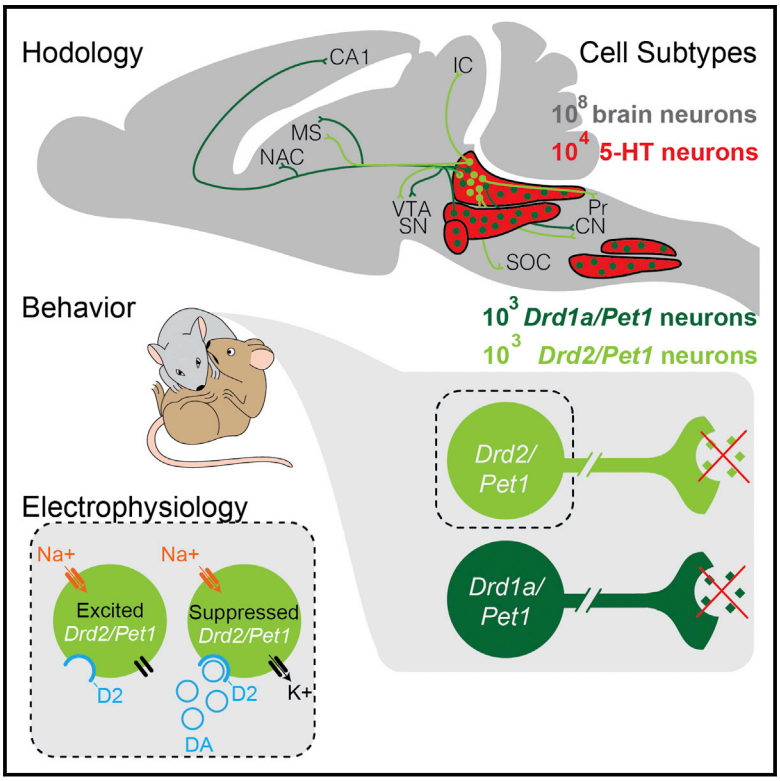

Authors

Vera Niederkofler, Tedi E. Asher, Benjamin W. Okaty, ..., Sheryl G. Beck, Klaus A. Miczek, Susan M. Dymecki

Correspondence

dymecki@genetics.med.harvard.edu

In Brief

Despite the established link between serotonin (5-HT) neurons and social behaviors, the specific neurons, circuits, and mechanisms mediating such relationships are unclear. Niederkofler et al. uncover and characterize two molecularly distinct subtypes of 5-HT neurons that influence mouse inter-male aggression levels and that may be selectively targetable pharmacotherapeutically.

Highlights

- Silencing serotonin (5-HT) neurons increases mouse inter-male aggression
- Aggression effects map to *Drd1a/Pet1* and *Drd2/Pet1* subtypes of 5-HT neurons
- DA regulates 5-HT neurons, inhibiting a subset via Drd2
- Axonal bouton mapping identifies neural targets of aggression-modulating subtypes

Accession Numbers

GSE87758

Niederkofler et al., 2016, Cell Reports *17*, 1934–1949
November 15, 2016
http://dx.doi.org/10.1016/j.celrep.2016.10.063

CellPress

OPEN ACCESS
CellPress

Cell Reports
Article

Identification of Serotonergic Neuronal Modules that Affect Aggressive Behavior

Vera Niederkofler,[1,5] Tedi E. Asher,[1,5] Benjamin W. Okaty,[1] Benjamin D. Rood,[1] Ankita Narayan,[1] Lara S. Hwa,[2] Sheryl G. Beck,[3,4] Klaus A. Miczek,[2] and Susan M. Dymecki[1,6,*]

[1]Department of Genetics, Harvard Medical School, 77 Avenue Louis Pasteur, Boston, MA 02115, USA
[2]Department of Psychology, Tufts University, 530 Boston Avenue, Medford, MA 02155, USA
[3]Departments of Anesthesiology and Critical Care and Pharmacology, Perelman School of Medicine at the University of Pennsylvania, Philadelphia, PA 19104
[4]Department of Anesthesiology and Critical Care, Children's Hospital of Philadelphia, Philadelphia, PA 19104, USA
[5]Co-first author
[6]Lead Contact
*Correspondence: dymecki@genetics.med.harvard.edu
http://dx.doi.org/10.1016/j.celrep.2016.10.063

SUMMARY

Escalated aggression can have devastating societal consequences, yet underlying neurobiological mechanisms are poorly understood. Here, we show significantly increased inter-male mouse aggression when neurotransmission is constitutively blocked from either of two subsets of serotonergic, *Pet1*$^{+}$ neurons: one identified by dopamine receptor D1(Drd1a)::cre-driven activity perinatally, and the other by *Drd2::cre* from pre-adolescence onward. Blocking neurotransmission from other Pet1^{+} neuron subsets of similar size and/or overlapping anatomical domains had no effect on aggression compared with controls, suggesting subtype-specific serotonergic neuron influences on aggression. Using established and novel intersectional genetic tools, we further characterized these subtypes across multiple parameters, showing both overlapping and distinct features in axonal projection targets, gene expression, electrophysiological properties, and effects on non-aggressive behaviors. Notably, Drd2::cre marked 5-HT neurons exhibited D2-dependent inhibitory responses to dopamine in slices, suggesting direct and specific interplay between inhibitory dopaminergic signaling and a serotonergic subpopulation. Thus, we identify specific serotonergic modules that shape aggression.

INTRODUCTION

Throughout the animal kingdom, species-typical aggressive behaviors are used to acquire or safeguard food, mating partners, progeny, and territory, and are essential for individual and population survival (Marler, 1976). Even though specific behavior patterns differ between species, the motivation toward aggression has been strongly conserved evolutionarily (Lorenz, 1966). Likewise, aggression is an inherent thread in the fabric of human society, but when escalated and uncontrolled, as can occur in disorders such as schizophrenia, intermittent explosive disorder, autism, or even dementia (Volavka, 2002), the outcome can be detrimental to the individual and society. Across these varied DSM-V (American Psychiatric Association, 2013) disease categories, the behavioral presentation of aggression is one integral endophenotype, perhaps reflecting a shared underlying component at the level of specific cells, circuits, and/or genes, as conceptually put forth by National Institute of Mental Health's (NIMH's) RDoC (Research Domain Criteria; https://www.nimh.nih.gov/research-priorities/rdoc/constructs/rdoc-matrix.shtml). Here we discriminate specific brain serotonergic neuronal subtypes linked to abnormally high levels of inter-male aggression in mice and analyze these neuronal modules across multiple levels (RDoC "units of analysis"), from the molecular and cellular to the organismal.

Motivating this work in part are the many pharmacological manipulations and gene association studies establishing serotonin (5-hydroxytryptamine, 5-HT) and the neurons that produce it as shaping aggression levels in animals and humans (Audero et al., 2013; Lesch and Merschdorf, 2000; Zalsman et al., 2011; Takahashi and Miczek, 2014). Increasingly, evidence points to an association between decreased serotonergic tone in the adult and an increased potential for pathological aggression (Hendricks et al., 2003; Takahashi and Miczek, 2014; Saudou et al., 1994; Audero et al., 2013; Angoa-Pérez et al., 2012; Mosienko et al., 2012; Alenina et al., 2009). In line, current treatments for patients displaying impulsive aggression include substances that enhance 5-HT levels, e.g., selective serotonin reuptake inhibitors (Bond, 2005; Coccaro and Kavoussi, 1997; Reist et al., 2003) or monoamine oxidase A inhibitors (Hollander, 1999). Such treatments, though, target the entire serotonergic neuronal system and thus can trigger undesirable and even dangerous side effects because of the multiplicity of behaviors and physiological processes modulated by 5-HT (reviewed in Hale et al., 2012 and Lucki, 1998). Increasing evidence suggests that the many functions modulated by the serotonergic system

are, at least partially, the collective result of distinct serotonergic neuronal modules, each governing a particular set of functions (Brust et al., 2014; Molliver, 1987; Fernandez et al., 2015; Gaspar and Lillesaar, 2012; Hale et al., 2012; Kim et al., 2009; Okaty et al., 2015). A key question, then, is whether there are specialized distinct serotonergic neurons that shape facets of aggression or whether instead, global changes in serotonergic tone are necessary.

Recent work has demonstrated the utility of subdividing the 5-HT neuronal system based on patterns of gene expression therein identifying distinct molecular subtypes of serotonergic neurons that can be targeted for functional studies (Brust et al., 2014; Spaethling et al., 2014; Commons et al., 2003; Fox and Deneris, 2012; Wylie et al., 2010; Fernandez et al., 2015; Jensen et al., 2008; Okaty et al., 2015). To test whether specialized serotonergic neurons involved in establishing normative levels of aggression exist, we implemented intersectional genetic strategies in mice (Awatramani et al., 2003; Jensen et al., 2008; Kim et al., 2009) to functionally silence molecularly defined subsets of serotonergic neurons and assess the effects on aggressive behavior. Resultant findings reveal functional modularity within the serotonergic neuronal system at the behavioral, cellular, and hodological levels, providing insight into the cellular and molecular substrates that may influence behaviors such as aggression.

RESULTS

Neurotransmission by Serotonergic Neurons Is Required for Normative Levels of Adult Inter-male Rodent Aggression

We employed molecular genetic tools to probe whether neurotransmission from serotonergic neurons is required for normative levels of aggressive behavior in adult male mice, and if so, to determine which subtypes of serotonergic neurons underlie this function. We ''silenced'' vesicular neurotransmission from 5-HT neurons constitutively through recombinase-dependent expression of a tetanus toxin light chain-GFP fusion, referred to throughout as ''tox'' (Kim et al., 2009), which impedes Vamp2-dependent exocytosis of neurotransmitters. We previously established tox as potent and effective in serotonergic neurons (Kim et al., 2009).

Using a double-transgenic strategy pairing the pan-serotonergic *ePet::cre* driver (Scott et al., 2005) with the Cre-responsive *RC::Ptox* allele (Kim et al., 2009) (Figure 1A), we observed robust and reproducible tox expression restricted to regions containing the serotonergic raphe nuclei in double-transgenic *ePet::cre, RC::Ptox* animals (referred to here as *Pet1*-silenced animals; Figure 1B), but not single-transgenic *RC::Ptox* control littermates (Figure 1C). Immunohistochemical analyses of brain tissue from double-transgenic *ePet::cre, RC::Ptox* mice further showed that 5-HT-positive axonal varicosities and synaptic boutons were diminished in VAMP2, consistent with VAMP2 cleavage by tox, the documented method of tetanus toxin light chain activity (Link et al., 1992; Kim et al., 2009) (Figures 1D and 1E). Additionally, serotonergic axonal processes in brains of *ePet::cre, RC::Ptox* mice appeared enlarged qualitatively (Figure 1D) relative to controls (Figure 1E), consistent with a buildup of 5-HT-loaded vesicles caused by disrupted release (Kim et al., 2009). Finally, microdialysis experiments (Figure 1F) sampling the medial prefrontal cortex (mPFC; Figure S1), a known projection target of serotonin neurons (Azmitia and Segal, 1978), demonstrated a near absence of extracellular 5-HT in *ePet::cre, RC::Ptox* transgenic mice at baseline (controls versus *ePet::cre, RC::Ptox*, Mann-Whitney U test (M-W U) < 0.0001, $p = 0.008$). Systemic administration of fenfluramine (3 mg/kg i.p. [intraperitoneally]), which has been shown to induce serotonin release via reversal of the serotonin transporter (Rothman et al., 2003), increased extracellular 5-HT in both *Pet1*-silenced and control siblings (main effect of time course $F(9, 119) = 17.1$; $p < 0.001$; Figure 1G), although serotonin levels remained higher in controls (main effect of genotype $F(1, 119) = 10.3$; $p = 0.009$). These data suggest that normal vesicular 5-HT release was blocked, but that viable axons were still present in the mPFC of *ePet::cre, RC::Ptox* mice.

To determine the impact of en masse silencing of serotonergic neurons on aggressive behaviors, we subjected individual *Pet1*-silenced mice and sibling controls to an ethologically guided version of the resident-intruder (R-I) assay (Fish et al., 1999; Miczek and O'Donnell, 1978) (Figure 1H). Each test mouse (resident male) was ''primed'' with a brief non-contact exposure to a male breeder, after which an intruder male was placed into the resident's home cage. This assay provided high enough baseline levels of aggression to detect increases or decreases (Miczek and O'Donnell, 1978; Fish et al., 1999).

Using this assay, *Pet1*-silenced mice displayed more aggression than control siblings. *Pet1*-silenced mice delivered significantly more attack bites (Figure 1I; 17.0 ± 1.7 [*Pet1*-silenced, $n = 10$] versus 8.1 ± 1.7 [control, non-*tox*-expressing siblings, $n = 20$]; M-W $U = 38$, $p = 0.005$; breakdown of sibling controls by single-transgenic genotype is shown in Figure S2A), displayed significantly more lateral threats toward intruders (30.1 ± 3.4 versus 15.6 ± 3.6; M-W $U = 51.5$, $p = 0.03$; Figure 1J), and spent significantly more time tail rattling than controls (3.5 ± 1.0 s versus 1.4 ± 0.4 s; M-W $U = 45$, $p = 0.01$; Table S1). Although *Pet1*-silenced mice tended to demonstrate their first attack bite sooner and to pursue intruders more often than controls, these differences did not reach statistical significance (Table S1).

These data are consistent with the model that functional deficiency in serotonergic neurons is associated with increased aggression (Hendricks et al., 2003; Audero et al., 2013; Angoa-Pérez et al., 2012; Mosienko et al., 2012; Alenina et al., 2009). The present findings further establish an experimental platform with which to delineate those serotonergic neurons that are responsible for these effects on aggression.

Specific Subtypes of Brain Serotonergic Neurons Shape Inter-male Aggression Levels

We used a dual-recombinase (Cre and Flpe)-based intersectional approach (Figure 2) (Jensen et al., 2008; Awatramani et al., 2003; Kim et al., 2009; Ray et al., 2011; Dymecki et al., 2010) to test whether there exist specialized aggression-influencing subtypes of serotonergic neurons. By leveraging molecular differences across serotonergic neurons to drive *tox* expression, we silenced discrete molecular subtypes of serotonergic

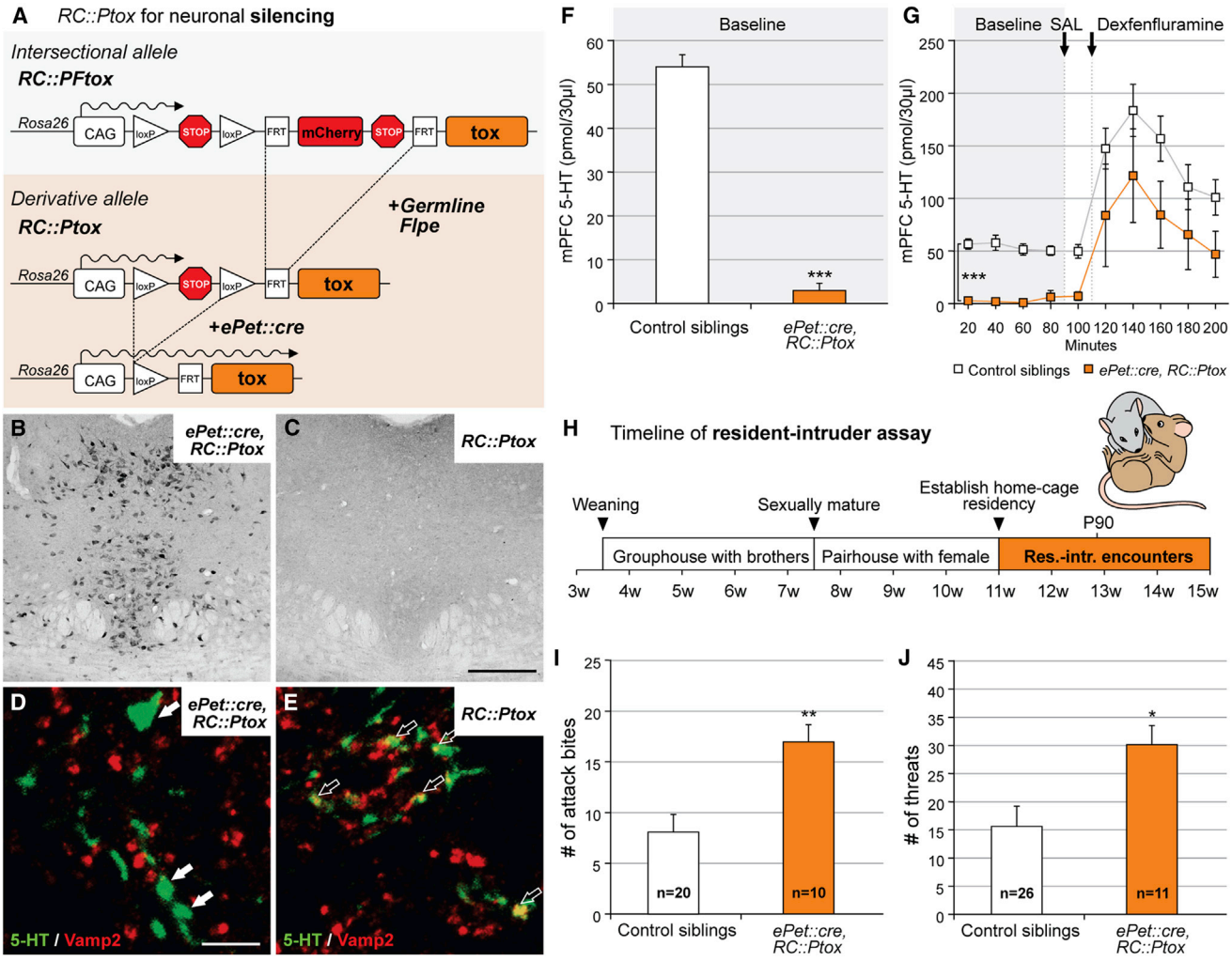

Figure 1. Silencing Serotonin Neurons En Masse Increases Aggression

(A) Schematic illustrates strategy for pan-serotonergic *tox*-mediated silencing. Silencing of *Pet1* neurons was accomplished by pairing *RC::Ptox,* a Cre-only responsive derivative allele of *RC::PFtox*, with the driver *ePet::cre*.

(B and C) Photomicrographs of the dorsal raphe showing immunostaining for GFP from *ePet::cre, RC::Ptox* (B) and *RC::Ptox* control (C) mice illustrate the effectiveness of tox-GFP fusion protein expression when *ePet::cre* is present. Scale bar, 500 µm.

(D and E) Serotonergic axon terminals in the trigeminal nucleus show that Vamp2 staining is absent from serotonergic terminals in *ePet::cre, RC::Ptox* mice (D, no yellow), but that immuno-labeled 5-HT and Vamp2 colocalize in *RC::Ptox* controls (E, yellow). Scale bar, 5 µm.

(F) As measured by in vivo microdialysis, baseline serotonin levels (mean ± SEM) in the mPFC were significantly lower in *ePet::cre, RC::Ptox* (orange) than in *RC::Ptox* (white) controls (M-W U < 0.0001, p = 0.008).

(G) 5-HT levels (mean ± SEM) in mPFC dialysate samples from *ePet::cre, RC::Ptox* (orange) and control (white) mice before and after administration of dexfenfluramine (3 mg/kg i.p.), which induces non-exocytotic release of neurotransmitter.

(H) Timeline of experimental design for resident-intruder assay illustrating rearing and housing conditions of male test subjects (residents).

(I) Number of attack bites (mean ± SEM) demonstrated by *ePet::cre, RC::Ptox* mice (orange) and control siblings (white) during the resident-intruder assays (M-W U = 38, p = 0.005).

(J) Number of lateral threats (mean ± SEM) demonstrated by *ePet::cre, RC::Ptox* mice (orange) and control siblings (white) during the resident-intruder assays (M-W U = 51.5, p = 0.03).

neurons and assayed the impact on aggression using the resident-intruder test described above.

To gain genetic access to molecular subsets of serotonergic neurons, we partnered the intersectional reporter allele *RC::FrePe* (Figure 2A) (Bang et al., 2012; Brust et al., 2014) or silencing allele *RC::PFtox* (Figure 2B) (Kim et al., 2009), respectively, with the pan-serotonergic *Pet1::Flpe* driver and one of multiple *cre* driver lines. We chose five *cre* drivers whose expression delineates subsets distributed throughout the serotonergic raphe nuclei. Three of these drivers (Gong et al., 2007) targeted subtypes with constituent neurons residing in the dorsal raphe nucleus (DR): *dopamine receptor type-I (Drd1a::cre)*, *dopamine receptor type-II (Drd2::cre)*, and *corticotropin-releasing factor (Crf::cre)*. We additionally selected two *cre* drivers, *r2Hoxa2::cre*

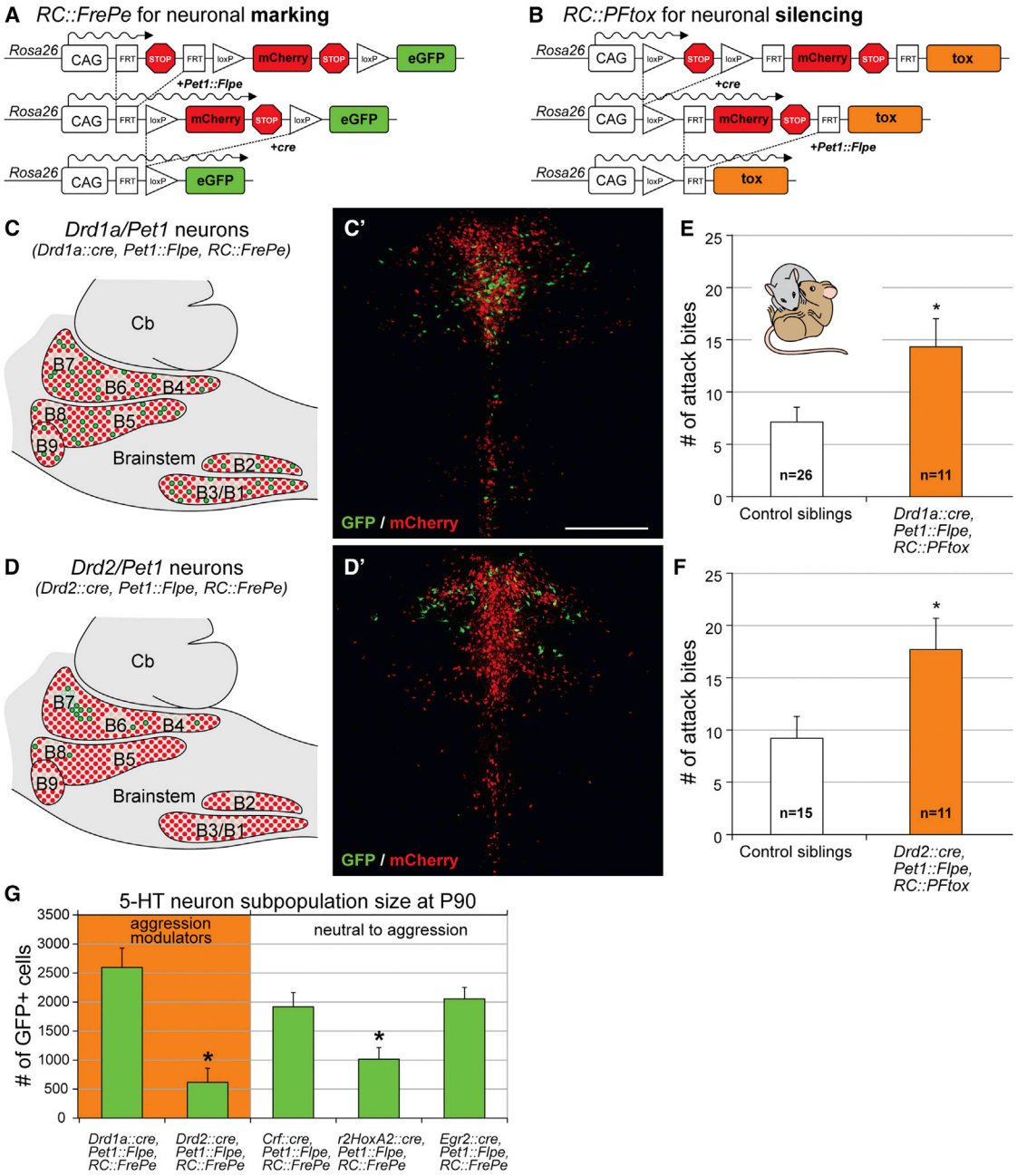

Figure 2. Serotonergic Subtypes that Modulate Aggression

(A and B) Schematics illustrate strategies for labeling (A) or silencing (B) subtypes of serotonergic neurons.

(C, C′, D, and D′) Cartoons of a sagittal brain slice illustrate the distributions of the *Drd1a/Pet1* (C) and *Drd2/Pet1* subtypes (D) within the serotonergic raphe (B1-B9). Photomicrographs show the presence of GFP$^+$ *Drd1a/Pet1* (C′) and GFP$^+$ *Drd2/Pet1* neurons (D′) within the context of the remaining *Pet1*$^+$ population labeled by mCherry in coronal brain slices through the DR (B7). Scale bar, 50 μm (C′).

(E and F) *Drd1a/Pet1*-silenced (E) and *Drd2/Pet1*-silenced (F) mice exhibited more attack bites than control siblings during the resident-intruder assay (*Drd1a/Pet1*: M-W U = 75, p = 0.023; *Drd2/Pet1*: M-W U = 42, p = 0.036).

(G) Number of GFP$^+$ neurons (mean ± SEM) for each of the five subtypes detected using the *RC::FrePe* reporter allele in the serotonergic raphe system of male mice (P90; one-way ANOVA, $F_{(4,10)} = 10.47$, p = 0.001, Fisher's LSD, $p < 0.05$).

Cb, cerebellum.

(Awatramani et al., 2003) and *Egr2::cre* (Voiculescu et al., 2000), which together encapsulate most median raphe (MR; also referred to as the prepontine raphe [PnR]; Alonso et al., 2013) and raphe magnus (RMg) neurons (Jensen et al., 2008), respectively. We refer to the captured intersectional neuron subtypes as *Drd1a/Pet1* (Figures 2C and C′), *Drd2/Pet1* (Figures 2D and 2D′),

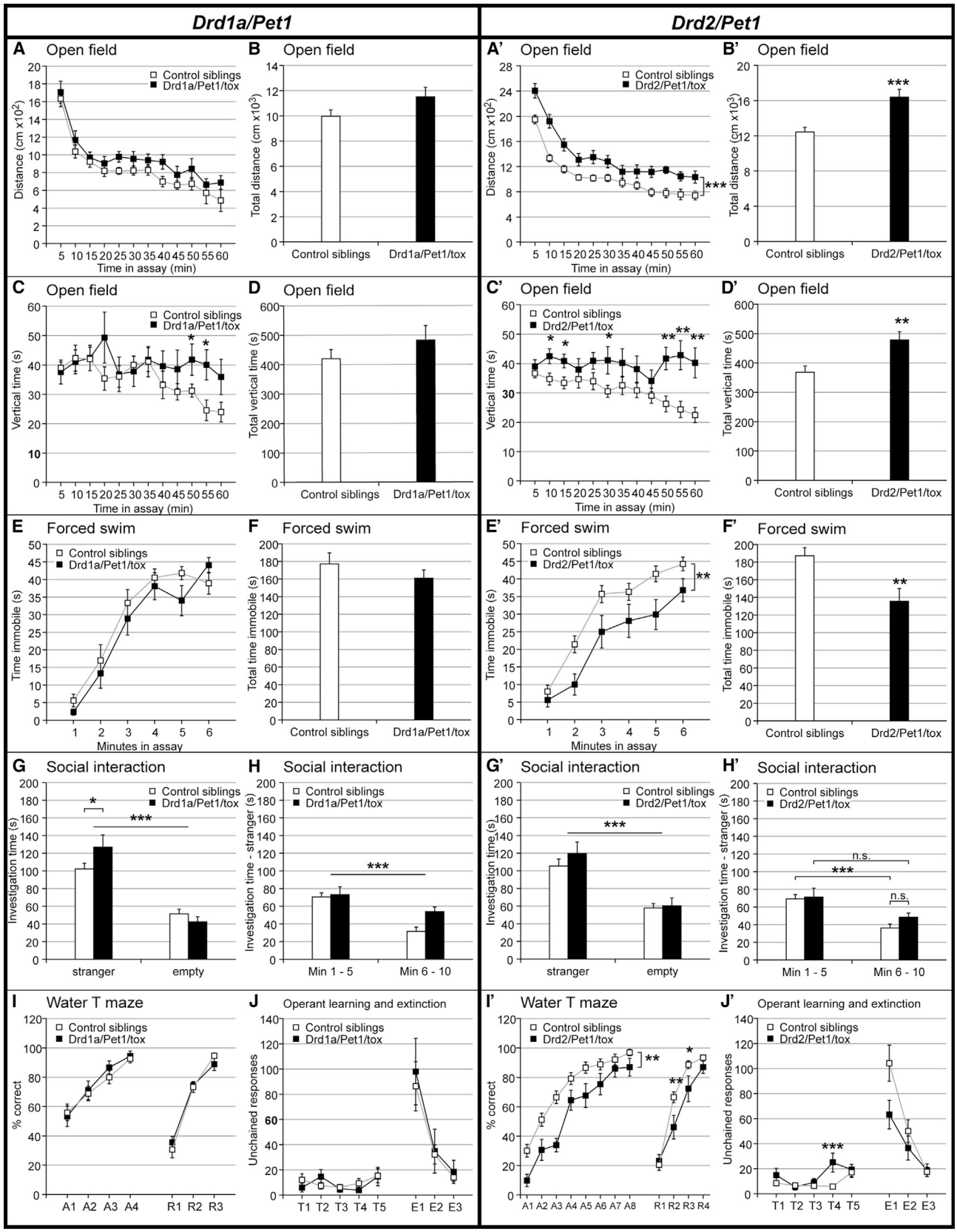

(legend on next page)

Crf/Pet1 (Figures S3A and S3A′), *r2Hoxa2/Pet1* (Figures S3B and S3B′), and *Egr2/Pet1* (Figures S3C and S3C′).

We analyzed the effect of tox-mediated silencing of each molecularly defined neuronal subtype. Silencing of either the *Drd1a/Pet1* or the *Drd2/Pet1* neuron subtypes resulted in an increase in number of attack bites compared with non-*tox*-expressing littermate controls (*Drd1a/Pet1*-silenced [n = 11]: 14.3 ± 2.7 attack bites, control siblings [n = 26]: 7.3 ± 1.4 attack bites, M-W U = 75, p = 0.023; *Drd2/Pet1*-silenced [n = 11]: 17.7 ± 3.0 attack bites, control siblings [n = 15]: 9.2 ± 2.2 attack bites, M-W U = 42, p = 0.036; Figures 2E and 2F; breakdown of controls by genotype shown in Figures S2B and S2C). By contrast, silencing of *Crf/Pet1* neurons (n = 12, 10.6 ± 3.1 attack bites), *r2HoxA2/Pet1* neurons (n = 11, 7.8 ± 1.7 attack bites), or *Egr2/Pet1* neurons (n = 12, 7.6 ± 2.1 attack bites) did not increase the number of attack bites relative to control siblings (*Crf/Pet1* controls: n = 22, 10.9 ± 1.7 attack bites, U = 170, p = 0.75; *r2HoxA2/Pet1* controls: n = 24, 4.5 ± 1.1 attack bites, M-W U = 94.5, p = 0.14; *Egr2/Pet1* controls: n = 23, 8.6 ± 1.8 attack bites, M-W U = 132.5, p = 0.85; Figures S3D–S3F and S4).

We next queried whether silencing of *Drd1a/Pet1* or *Drd2/Pet1* neurons affected other aspects of aggressive behavior (Table S2). We observed a significant increase in the number of lateral threats when we silenced either of the two subtypes (*Drd1a/Pet1-silenced*: 26.6 ± 4.8 versus control siblings: 13.8 ± 2.9, M-W U = 76.5, p = 0.025; *Drd2/Pet1-silenced*: 34.5 ± 6.3 versus control siblings: 15.0 ± 3.5, M-W U = 36, p = 0.017). *Drd1a/Pet1*-silenced mice (90.8 ± 25.5 s) also had a significantly shorter average latency to attack than respective sibling controls (171.9 ± 22.9 s, M-W U = 82.5, p = 0.046). Silencing either subtype failed to affect time spent tail rattling or number of pursuits. These data show that the *Drd1a/Pet1* and *Drd2/Pet1* subtypes of serotonergic neurons influence some, but not all, salient elements of rodent aggressive behaviors.

To rule out that the observed aggression phenotypes might result from silencing a sufficiently large number of non-specific serotonergic neurons, we quantified the cell population size of each of the *Pet1* neuron subsets tested in the resident-intruder assay. We counted the number of GFP^+ cells in the brains of male mice generated by pairing *RC::FrePe* with *Pet1::Flpe* and subtype-specific *cre* drivers. We found that the *Drd1a/Pet1*, *Crf/Pet1*, and *Egr2/Pet1* subsets were of comparable size with 2594 ± 333, 1918 ± 247, and 2052 ± 200 GFP^+ cells per brain, respectively (Figure 2G). The *Drd2/Pet1* and *r2HoxA2/Pet1* subsets were significantly smaller with 616 ± 241 and 1016 ± 199 GFP^+ cells per brain, respectively (one-way ANOVA, genotype $F_{(4,10)} = 10.47$, p = 0.001, Fisher's least significant difference [LSD], $p < 0.05$; Figure 2G). The aggression-relevant *Drd2/Pet1* subset was the smallest serotonergic population tested, indicating that the observed aggression phenotypes were not the result of silencing a threshold number of non-specific serotonergic neurons, but rather resulted from silencing distinct serotonergic neuron subtypes.

Drd1a/Pet1 and *Drd2/Pet1* Neurons Modulate Unique Sets of Non-aggressive Behavior

We next investigated the broader role these neuron subtypes play in regulation of motor and emotionally relevant behavior. We quantified non-aggressive behaviors during the resident-intruder assays and found that *Drd1a/Pet1*-silenced mice spent significantly less time making "nose-to-nose" and "nose-to-anogenital region" contacts with the intruder (*Drd1a/Pet1-silenced*: 2.5 ± 0.7 s, control siblings: 7.2 ± 1.0 s [mean ± SEM]; M-W U = 48, p = 0.002) and significantly more time walking around the cage compared with control siblings (*Drd1a/Pet1*-silenced: 110.7 ± 6.4 s, control siblings: 91.8 ± 3.4 s; M-W U = 67, p = 0.016). *Drd1a/Pet1*-silenced mice did not differ significantly from controls in rearing, digging, or grooming behaviors (Table S3). No changes in non-aggressive behaviors during the resident-intruder assay were detected in *Drd2/Pet1*-silenced mice (Table S3).

Further, we subjected new cohorts of *Drd1a/Pet1*- and *Drd2/Pet1*-silenced mice and their control littermates to behavioral assays assessing neurological functions, emotional responses, social behavior, and cognitive functions (Figures 3 and S5; Tables S4 and S5). Although the *Drd2/Pet1* subset is significantly smaller in neuron number and more circumscribed anatomically than the *Drd1a/Pet1* subset, *Drd2/Pet1* silencing affected a wider range of behavioral outcomes. *Drd1a/Pet1*-silenced males demonstrated subtle, yet statistically significant, phenotypes in 2 of the 10 tests (open-field and social interaction tests; Figures 3A–3J), whereas *Drd2/Pet1*-silenced males showed a relatively robust array of behavioral phenotypes in 4 of the 10 tests (open-field, forced swim test, water T-maze, and operant learning; Figures 3A′–3J′). See Tables S4 and S5 for statistical analysis of behavioral assays. Both *Drd1a/Pet1*- and *Drd2/Pet1*-silenced mice exhibited hyperactivity in novel environments, although the phenotype was more evident in the *Drd2/Pet1*-silenced animals (Figures 3A–3D and 3A′–3D′). *Drd2/Pet1*-silenced mice also demonstrated hyperactivity in the forced swim test and hyperactivity or impulsivity in the water T-maze and operant learning assays (Figures 3E′, 3F′, 3I′, and

Figure 3. Behavioral Phenotyping of *Drd1a/Pet1*- and *Drd2/Pet1*-Silenced Mice

(A–D and A′–D′) Open field. Horizontal distance traveled during a 60 min open field assay is shown in 5 min bins (A and A′) and as total distance traveled (B and B′). Time spent in vertical exploration is shown in 5 min bins (C and C′) and as total vertical exploration time (D and D′).

(E, E′, F, and F′) Forced swim. Average time spent immobile during each minute of the forced swim test (E and E′) and the total time spent immobile (F and F′).

(G, G′, H, and H′) Three-chamber social interaction. (G and G′) Average time spent investigating the perforated container holding a stranger mouse (under perforated cup) or investigating an empty perforated container during the three-chamber social interaction assay. (H and H′) Average time spent at the container with the stranger mouse binned into first and second halves of the assay is shown.

(I and I′) Water T-maze. The graphs plot the % of correct arm choices during acquisition and reversal learning phases for *Drd1a/Pet1*-silenced (I), *Drd2/Pet1*-silenced (I′), and control mice.

(J and J′) Operant learning task. The graphs plot the number of unchained responses, lever presses in the absence of stimuli, during training, and extinction phases for the *Drd1a/Pet1*-silenced (J), *Drd2/Pet1*-silenced (J′), and control mice.

All values shown are mean ± SEM. Complete statistical measures are provided in Tables S4 (*Drd1a/Pet1*) and S5 (*Drd2/Pet1*).

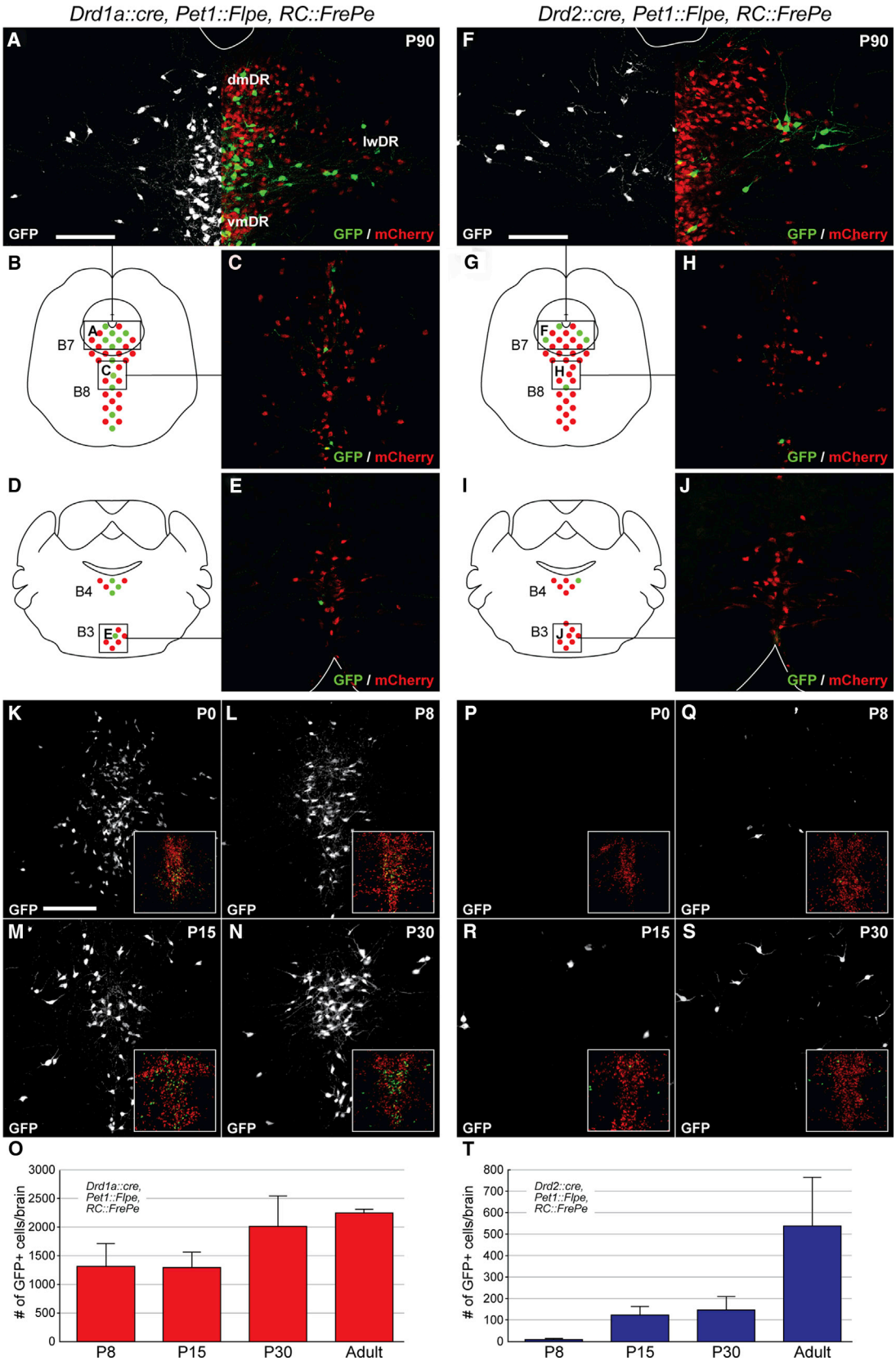

(legend on next page)

3J′). *Drd1a*/*Pet1*-silenced mice did not show phenotypes in these assays, but spent significantly more time with the stranger mouse in the social interaction test as compared with sibling controls (Figures 3G and 3H). These results suggest that *Drd2*/*Pet1*-silenced animals exhibit more persistent motor activity in a novel environment, but not in the home cage, as well as potentially impaired spatial learning ability. By contrast, *Drd1a*/*Pet1*-silenced mice demonstrate only slight hyperactivity and increased social preference.

Drd1a/Pet1 and *Drd2/Pet1* Neuron Subtypes Differ in Anatomical Distribution and Onset of Respective *Drd::cre* Expression

We next examined *Drd1a*/*Pet1* and *Drd2*/*Pet1* neuron distribution across the serotonergic raphe. The DR (composed of nuclei B7, B6, and B4 [Dahlstroem and Fuxe, 1964; Steinbusch, 1981], with B4 here considered the caudal-most DR domain) can be broken down into the ventromedial (vmDR), dorsomedial (dmDR), and lateral wing regions (Hale and Lowry, 2011; Peyron et al., 1995). In the adult brain, *Drd1a*/*Pet1* neurons were detected throughout raphe nuclei largely enriched along the midline (Figures 4A–4E). By contrast, *Drd2*/*Pet1* neurons localized to the rostral-most DR (B7; Figures 4F–4J), especially the lateral wings (Figures 4A and 4F), with few cells in the caudal DR, MR (B8), and medullary raphe (B3, RMg).

Because intersectional reporter expression served as a proxy for the onset of putative *dopamine receptor* gene and *tox* expression, we examined the ontogeny of GFP expression driven by *RC::FrePe*. *Pet1* and *Pet1::Flpe* expression begins in the newly postmitotic precursor serotonin neurons around embryonic day (E) 12.5 (Jensen et al., 2008; Scott et al., 2005), with *Drd* expression subsequently. We detected *Drd1a*/*Pet1* GFP$^+$ cells in late-gestation embryos (data not shown), with numerous marked cells by post-natal day (P) 0 (Figure 4K) and increasing at later ages (Figures 4K–4O). By contrast, *Drd2*/*Pet1* GFP$^+$ neurons were observed starting around P8, were consistently detectable by P15, and increased in number between P30 and adulthood (Figures 4P–4T). Thus, although a considerable number of *Drd1a*/*Pet1* neurons demonstrated Cre activity embryonically, most *Drd2*/*Pet1* neurons showed Cre activity (and thus GFP and tox expression) only later during post-natal development (i.e., P8 and later).

Drd2/Pet1 Neurons Express Functional D2 Receptors

To determine whether dopamine receptor genes are indeed expressed in the adult *Drd1a*/*Pet1* and *Drd2*/*Pet1* cell populations, we manually sorted fluorescently labeled cells (Hempel et al., 2007) from the DR of adult triple-transgenic mice. RNA was extracted from single cells and, in the case of *Drd1a*/*Pet1* mice, a pooled cell sample (~30 cells). The presence of endogenous *Drd1a* and *Drd2* transcripts as well as select pan-serotonergic marker genes was assessed using qRT-PCR and/or RNA sequencing (RNA-seq).

Using RNA-seq, we readily detected *Drd2* transcripts in 17 of 17 cells, with 16 of 17 having a counts per million read (CPM; Anders et al., 2013) greater than 1, a commonly applied detection threshold (Figure 5A). To determine whether the *Drd2::cre* driver was capturing near all *Drd2*-expressing 5-HT neurons, we also measured gene expression in eight mCherry$^+$ *Pet1*-only neurons. Three of eight *Pet1*-only cells had a *Drd2* CPM > 1, only one of which was above the lower quartile range of *Drd2* transcript expression levels in *Drd2*/*Pet1* GFP$^+$ cells (Figure 5A). Applying a generalized linear model likelihood ratio test using edgeR (Anders et al., 2013), we confirmed that transcript counts were significantly greater in the *Drd2*/*Pet1* sample group than in the *Pet1*-only group ($p = 0.03$) by a factor of 6. By contrast, select 5-HT marker transcripts including *tryptophan hydroxylase 2* (*Tph2*), *serotonin transporter* (*Slc6a4*, also referred to as *Sert*), and *Pet1* were detected in all GFP$^+$ and mCherry$^+$ neurons by RNA-seq (Figures 5B and 5C). Together, these data indicate that the *Drd2*/*Pet1* neurons are bona fide serotonergic neurons that express endogenous *Drd2* transcripts. Transcripts for *Drd1a*, *Drd3*, *Drd4*, and *Drd5* were not detected in *Drd2*/*Pet1* GFP$^+$ neurons by RNA-seq (data not shown). Our data further show that the few *Pet1*-only neurons that harbor *Drd2* transcripts do so at significantly lower levels (close to the detection limit by RNA-seq), suggesting there may be a critical threshold of *Drd2* transcriptional activity to effectively drive the *Drd2::cre* transgene and perhaps to drive functionally meaningful levels of Drd2 receptor protein.

We next examined whether *Drd2*/*Pet1* neurons contained functional Drd2 receptors. We obtained whole-cell electrophysiological recordings from *Drd2*/*Pet1* (GFP$^+$) and *Pet1*-only (mCherry$^+$) neurons. In voltage clamp recordings from GFP$^+$

Figure 4. Reporter Labeling of Intersectional and Subtractive Serotonin Neuron Populations

Intersectional *Drd1a*/*Pet1* and *Drd2*/*Pet1* neurons express GFP, whereas the subtractive population of 5-HT neurons (*Pet1*-only) expresses mCherry, as labeled by the intersectional reporter *RC::FrePe*.

(A–C) Images show *Drd1a*/*Pet1* GFP$^+$ and *Pet1*-only mCherry$^+$ neurons from regions of the DR (A) and MR (C) as diagrammed in (B). (A) The left side of the image shows in white *Drd1a*/*Pet1* neurons, and the right half shows both *Drd1a*/*Pet* (green) and *Pet1*-only (red) neurons. (A and F) White line delineates the cerebral aqueduct. Scale bars, 50 μm.

(D and E) Drawing (D) illustrates the brain section from which the RMg was imaged (E). White line delineates ventral brain surface.

(F–H) Images show *Drd2*/*Pet1* GFP$^+$ and *Pet1*-only mCherry$^+$ neurons from regions of the DR (F) and MR (H) as diagrammed in (G). (F) Left side of the image shows in white only the *Drd2*/*Pet1* neurons, and the right half shows both *Drd2*/*Pet1* and *Pet1* neurons. White line delineates cerebral aqueduct.

(I and J) Drawing (I) illustrates the brain section from which the RMg was imaged (J). White line delineates the ventral brain surface.

(K–N) Images show *Drd1a*/*Pet1* GFP$^+$ neurons within the DR of mice at P0 (K), P8 (L), P15 (M), and P30 (N). Insets show same region labeled with GFP and mCherry.

(O) Average number (mean ± SEM) of GFP$^+$ *Drd1a*/*Pet1* neurons within the DR at P8, P15, P30, and adult (>P90).

(P–S) Images show *Drd2*/*Pet1* GFP$^+$ neurons within the DR of mice at P0 (P), P8 (Q), P15 (R), and P30 (S). Insets show the same region labeled with GFP and mCherry.

(T) Average number (mean ± SEM) of GFP$^+$ *Drd2*/*Pet1* neurons within the DR at P8, P15, P30, and adult (>P90).

dm, dorsomedial; lw, lateral wings; vm, ventromedial.

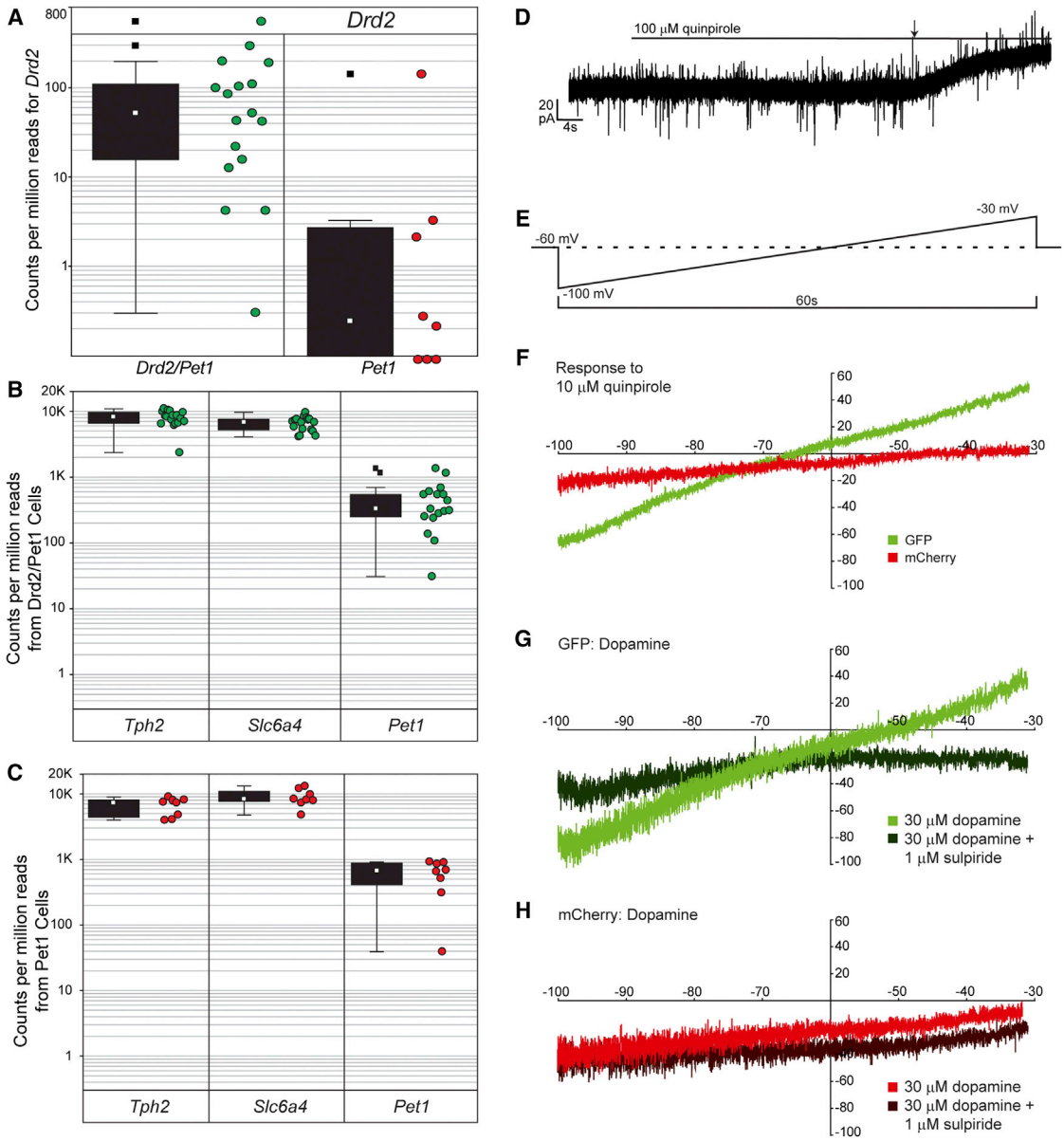

Figure 5. Validation of Dopamine Receptor Expression and Function

(A) Counts per million reads (CPM) for *Drd2* as measured using RNA-seq in *Drd2*/*Pet1* and *Pet1*-only neurons. Boxplots show the median (open square), upper and lower quartiles (box), non-outlier minimum/maximum (whiskers), and outliers (filled square). The associated raw data (green and red dots) are shown to the right of the boxplots.

(B) Boxplots show summaries and raw data of RNA-seq CPMs for three serotonergic marker genes expressed by the *Drd2*/*Pet1* neurons shown in (A): *tryptophan hydroxylase 2* (*Tph2*), *5-HT transporter* (*Slc6a4*), and *Pet1*.

(C) Boxplots show summaries and raw data of RNA-seq CPMs for *Tph2*, *Slc6a4*, and *Pet1* expressed by the *Pet1*-only neurons shown in (A).

(D) An example trace from a GFP$^+$ *Drd2*/*Pet1* neuron shows outward positive current elicited by bath application of 100 μM quinpirole, a D2-like receptor agonist. The line indicates when quinpirole was added to artificial cerebrospinal fluid (ACSF) reservoir, and the arrow indicates beginning of the response.

(E) Schematic illustrates ramp protocol employed before and after drug exposure to further explore the pharmacological responses to quinpirole and dopamine. From the holding potential of −60 mV, the membrane potential was dropped to −100 mV, raised over the course of 1 min to −30 mV, and then stepped back to −60 mV. To isolate drug-induced current, pre-drug ramps were subtracted from post-drug ramps.

(F) Shown are average current responses to 10 μM quinpirole for GFP$^+$ *Drd2*/*Pet1* (n = 8) and mCherry$^+$ *Pet1*-only (n = 5) neurons.

(G) Average current responses (Post − Pre) are shown for dopamine alone (light) and dopamine (30 μM) in the presence of the D2-like receptor antagonist sulpiride (1 μM, dark) for *Drd2*/*Pet1* neurons (n = 4).

(H) Average current responses (Post − Pre) are shown for dopamine (30 μM) alone (light) versus in the presence of sulpiride (1 μM, dark) for mCherry$^+$ *Pet1*-only neurons (n = 4).

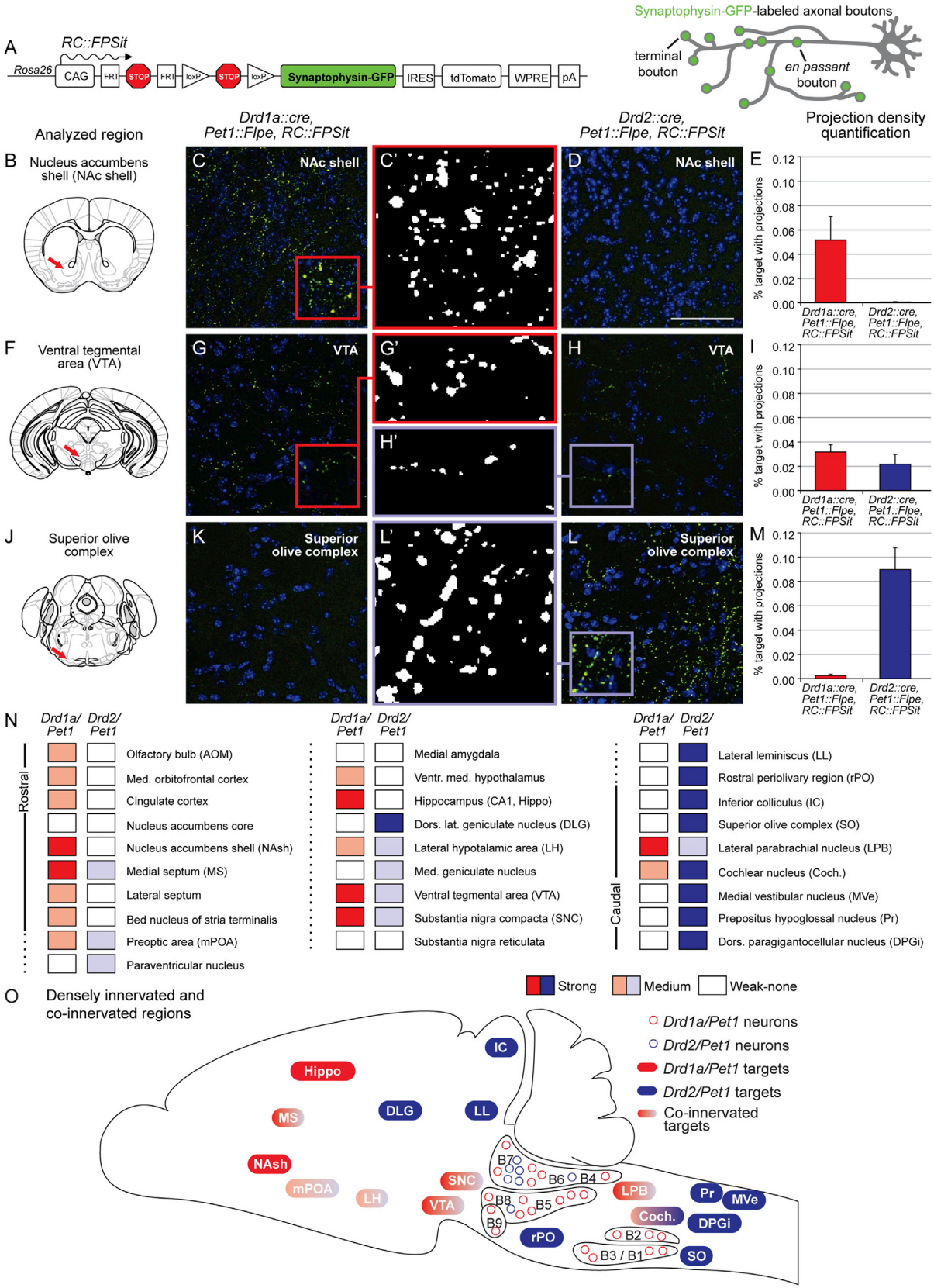

(legend on next page)

Drd2/Pet1 neurons, bath application of the D2 receptor agonist quinpirole (100 μM), which targets Drd2, Drd3, and Drd4, induced a small outward positive current (5.4 ± 2.3 pA, one-sample t test against $H_0 = 0$, n = 13, t = 2.38, p = 0.034; Figure 5D). Because recordings were carried out in the presence of glutamate and $GABA_A$ receptor antagonists and a blocker of voltage-gated sodium channels, the data suggest that the change in current observed was a direct response.

We next examined current change in response to a voltage ramp (−100 to −30 mV over 1 min; Figure 5E), before and after drug application for both GFP$^+$ *Drd2/Pet1* (n = 8) and mCherry+ *Pet1*-only (n = 5) neurons. The drug-specific response was calculated by subtracting pre- from post-drug ramp-induced current. GFP$^+$ *Drd2/Pet1* neurons, but not mCherry$^+$ *Pet1*-only neurons, demonstrated a voltage-dependent response to administration of 10 μM quinpirole: at low voltages, GFP$^+$ neurons showed a positive inward (excitatory) current, whereas at voltages greater than ∼−65 mV, they showed a positive outward (inhibitory) current (Figure 5F). The nature of the quinpirole-induced GFP$^+$ neuron response suggests the activation of a G-protein-coupled inwardly rectifying potassium channel (GIRK; Lesage et al., 1994; Sahlholm et al., 2008).

Administration of 30 μM dopamine recapitulated the quinpirole-induced response in GFP$^+$ *Drd2/Pet1* (Figure 5G), but not mCherry$^+$ *Pet1*-only neurons (Figure 5H). This current response in GFP$^+$ neurons was blocked by the D2 antagonist sulpiride (1 μM), which abrogated the positive outward current at depolarizing membrane potentials, indicating that the GIRK-like response was mediated by D2 receptors. These data indicate that *Drd2/Pet1* neurons express functional D2 receptors, which mediate an inhibitory effect on this neuronal subtype. The low levels of *Drd2* transcript detected in some mCherry$^+$ *Pet1*-only neurons is likely insufficient to drive functional protein expression. Interestingly, in both GFP$^+$ and mCherry$^+$ neurons, a positive inward current persisted in the presence of dopamine and sulpiride, suggesting that dopamine also had an excitatory effect (direct or indirect) on serotonergic neurons that was D2 independent.

In contrast with *Drd2/Pet1* neurons, *Drd1a* expression in *Drd1a/Pet1* GFP-marked neurons was ambiguous. We analyzed 23 individual GFP$^+$ *Drd1a/Pet1* cells derived from three adult *Drd1a::cre, Pet1::Flpe, RC::FrePe* animals (Table S6), as well as a pool of ∼30 GFP$^+$ cells from a fourth animal. qRT-PCR and RNA-seq revealed *Drd1a* transcript in the pooled sample, but not the single cells. Most samples also expressed *Tph2*, *Sert*, and *Pet1.* These data suggest that either *Drd1a* was not expressed by GFP$^+$ *Drd1a/Pet1* cells in adult animals (or expressed in only a very small number of cells) or expression levels were below our detection limit.

Because *Drd1a/Pet1* GFP$^+$ neurons are observed perinatally, we examined *Drd1a* transcript levels in single *Drd1a/Pet1* neurons from P4 (n = 4) and P10 (n = 8) pups (Table S7). Reads for *Drd1a* were observed in one of four cells at P4 and four of eight cells at P10, but only two of the P10 cells had CPM > 1. All 12 cells expressed *Tph2*, *Sert*, and *Pet1*. It is possible that some DR serotonergic neurons marked by the *Drd1a::cre* driver reflect ectopic transgene expression; however, because GFP serves as a permanent lineage tracer, *Drd1a* could be expressed largely transiently during development and downregulated by adulthood, as supported by our increased single-cell *Drd1* transcript detection frequency at earlier ages.

Low levels of *Drd2* transcript were detected in 8 of the 35 *Drd1a/Pet1* neurons assayed across all ages (Tables S6 and S7), suggesting that there may be some overlap between the two serotonergic neuronal lineages during adulthood, and that this sub-subtype may contribute to the shared behavioral phenotypes observed in our neurotransmission silencing experiments. We thus further explored and compared other aspects of cell phenotype between the two lineage-marked populations that might indicate shared versus divergent mechanisms of behavioral regulation, specifically axonal projection patterns.

Drd1a/Pet1 and *Drd2/Pet1* Neuron Subtypes Exhibit Unique Axonal Bouton Distribution Profiles

We mapped axonal projections of the *Drd1a/Pet1* and *Drd2/Pet1* neuron subtypes, using our engineered *ROSA26* knockin intersectional allele, *RC::FPSit* (Figure 6A), which labels axonal boutons (terminal and en passant) of a given neuron subtype with the presynaptic marker synaptophysin-GFP (Li et al., 2010). Some brain regions were innervated only by the *Drd1a/Pet1* subtype (Figures 6B–6E), some by both subtypes (Figures 6F–6I), and others only by the *Drd2/Pet1* subtype (Figures 6J–6M).

Figure 6. Axonal Projection Patterns of *Drd1a/Pet1* and *Drd2/Pet1* Neurons

(A) The *ROSA26/CAG* knockin allele, *RC::FPSit*, allows for visualization of subtype-specific axonal terminals with intersectionally expressed synaptophysin-GFP.

(B–E) Some areas, such as the nucleus accumbens (NAc) shell, were innervated by *Drd1a/Pet1* neurons, but not the *Drd2/Pet1* population. Schematic (B) illustrates the coronal section from which photomicrographs were taken for *Drd1a/Pet1* (C) and *Drd2/Pet1* (D) mice. In each image, GFP (green) and DAPI (blue) staining are shown. Center panel (C′) shows thresholded GFP$^+$ axonal terminals from the *Drd1a/Pet1* subtype, whereas (E) shows quantification of the area covered by GFP$^+$ staining (average % target area with projections). Scale bar, 50 μM.

(F–I) A few regions were innervated by both subtypes as in the ventral tegmental area (VTA). Schematic (F) indicates region analyzed. Representative images from *Drd1a/Pet1* (G) and *Drd2/Pet1* (H) mice demonstrate GFP$^+$ puncta in the VTA of both genotypes, as is depicted in the respective thresholded images (G′ and H′). Quantification of the area covered by GFP$^+$ staining is shown in (I).

(J–M) Other regions were innervated only by the *Drd2/Pet1* population as in the superior olivary complex (SO). Schematic (J) indicates the region analyzed. Representative images from *Drd1a/Pet1* (K) and *Drd2/Pet1* (L and L′) mice demonstrate GFP$^+$ puncta in the SO of *Drd2/Pet1*, but not *Drd1a/Pet1*, mice. Quantification of the area covered by GFP$^+$ staining is shown in (M).

(N) The binned level of innervation for the 28 brain regions analyzed in *Drd1a/Pet1* and *Drd2/Pet1* brains is indicated with white (no innervation, <0.005% coverage), light (weak innervation, 0.005%–0.03% coverage), or dark (strong innervation, >0.03% coverage) shading. Actual percentages are provided in Figure S4.

(O) In a sagittal representation, the densest areas of innervation and areas of co-innervation are shown for the *Drd1a/Pet1* (red shades) and *Drd2/Pet1* (blue shades) neuron subtypes. As in (N), light shades represent modest innervation, and dark shades represent dense innervation.

Apparent in adult (P90) brains from male triple-transgenic *Drd1a::cre, Pet1::Flpe, RC::FPSit* or *Drd2::cre, Pet1::Flpe, RC::FPSit* animals was that both subsets innervated numerous brain targets despite their small population size (Figures 6N, 6O, and S6). Based on a qualitative examination of innervation patterns, we chose for quantitative analyses 28 brain regions encompassing domains innervated by either the *Drd1a*/*Pet1* and/or *Drd2*/*Pet1* subtypes. We developed a largely automated imaging workflow that allowed for objective quantitative comparison of innervation density across different brains regions. Based on this output (Figure S6), we binned the analyzed target areas into categories of strong, medium, and weak-to-no-innervation (Figure 6N). We found that *Drd1a*/*Pet1* neurons projected strongly to forebrain nuclei, many of which are part of aggression circuits (Figures 6B–6I, 6N, 6O, and S6). By contrast, *Drd2*/*Pet1* neurons most prominently innervated more caudal brain areas, especially areas known to be involved in sensory (largely auditory) processing (Figures 6L, 6M, 6N, 6O, and S6). Some areas were co-innervated by *Drd1a*/*Pet1* and *Drd2*/*Pet1* (Figures 6F–6I, 6N, 6O, and S6).

DISCUSSION

Here we report discovery of two molecularly defined subtypes of serotonergic neurons, each critical for shaping aggressive social interactions in the mouse. One *Pet1* serotonergic cell subtype is distinguished by *Drd2::cre* driver activity from pre-adolescence onward and endogenous *Drd2* expression, and the other by *Drd1a::cre* activity perinatally with detectable endogenous *Drd1a* transcript in some, but not all, reporter-marked cells. Silencing of other subsets of serotonergic neurons, some of larger population size, did not affect aggressive behavior, indicating that constitutive silencing only of specific subtypes of serotonin neurons is sufficient to escalate adult male aggression. The *Drd2*/*Pet1* and *Drd1a*/*Pet1* subtypes are composed of remarkably few neurons, yet their axonal projections reach a broad range of targets. Differences between these subtypes in anatomical distribution, molecular expression, temporal onset of BAC-driven Cre activity, and projection profile suggest that they may modulate aggression through distinct mechanisms. Collectively, this work reveals the existence of molecularly, hodologically, and developmentally distinct subtypes of serotonergic neurons that are uniquely capable of influencing inter-male aggression.

Functional and Anatomical Differences between Aggression-Modulating 5-HT Neuron Subtypes

Silencing either the *Drd1a*/*Pet1* or the *Drd2*/*Pet1* subset of serotonergic neurons resulted in increased displays of aggressive behaviors in adult male mice, suggesting a model in which vesicular neurotransmission from these specific neuron subtypes, either during development and/or adulthood, is required to achieve normative, tempered levels of aggression in the adult.

Silencing of the *Drd2*/*Pet1* subtype further resulted in some form of hyper-arousal induced by novel or stressful environments. Because overall home cage activity measurement was unchanged, a generic motor phenotype is unlikely. By contrast, the *Drd1a*/*Pet1*-silenced animals displayed a phenotype in the social interaction assay, which may implicate the *Drd1a*/*Pet1* subtype in the regulation of social behaviors more generally. These differences in behavioral phenotypes may reflect distinctions observed between the two subtypes in anatomy, dopamine receptor gene expression, and projection targets.

We found that the two subtypes share some anatomical domains (largely the rostral dorsal DR), but largely differ in distribution within the raphe. The developmental onset of the respective *Drd::cre* drivers also differed between the *Drd1a*/*Pet1* and *Drd2*/*Pet1* subtypes. These findings suggest that although tox-mediated silencing is constitutive, its onset differed between the subtypes. While *Drd1a*/*Pet1* neuron labeling/silencing commenced embryonically, that for *Drd2*/*Pet1* neurons began at adolescence. Adolescence in mice is associated with functional changes in DR serotonin neurons and has been identified as a sensitive period for 5-HT-mediated modulation of emotional behavior in mice (Gross et al., 2002; Yu et al., 2014; Liu et al., 2010; Rood et al., 2014). From our present data, we can deduce that embryonic or early post-natal silencing of the *Drd2*/*Pet1* neurons is not necessary to induce behavioral phenotypes, but rather that subtype-specific neuronal silencing during later post-natal periods is sufficient.

Despite these differences, we observed some overlap between the subtypes, suggesting that the shared aggression phenotype upon neuronal silencing could stem from a neuronal sub-subtype denoted by a history of expression of *Pet1*/*Drd1a*/*Drd2*. However, the extent of these shared features was limited: *Drd2* transcript levels in *Drd1a*/*Pet1* cells are lower than those in *Drd2*/*Pet1* cells proper, while the shared anatomical and hodological properties are also a limited minority. Probing these *Pet1*/*Drd1a*/*Drd2*^{low} cells for a role in aggression modulation requires new tools with even greater cell subtype resolution.

Projection Targets of Aggression-Relevant *Drd1a/Pet1* and *Drd2/Pet1* Serotonergic Neurons

We developed a dual-recombinase allele, *RC::FPSit*, coding for a synaptophysin-GFP fusion protein enabling bouton visualization and thus enhancing subtype innervation mapping. Several of the innervated brain regions have documented roles in modulating aggressive behavior (Nelson and Trainor, 2007) or contain dopaminergic neuron cell bodies. *Drd1a*/*Pet1* neurons mostly innervated rostral brain structures known to constitute aggression circuits, whereas *Drd2*/*Pet1* projection targets showed a surprising caudal bias. The majority were centers associated with auditory processing. Notably, some human disorders associated with 5-HT dysregulation involve sound hypersensitivity or aberrant auditory processing (Kähkönen et al., 2007; Lucker and Doman, 2012; Wyss et al., 2013). Thus, the behavioral phenotypes in the *Drd2*/*Pet1*-silenced animals could be related to altered sensory processing. Importantly, *Drd2*/*Pet1*-silenced mice exhibited a normal startle reflex, suggesting that hearing is not overtly impaired. Overall, projection targets of the *Drd1a*/*Pet1* and *Drd2*/*Pet1* neuron subtypes differ considerably, possibly reflecting distinct circuits through which each subset influences behavior.

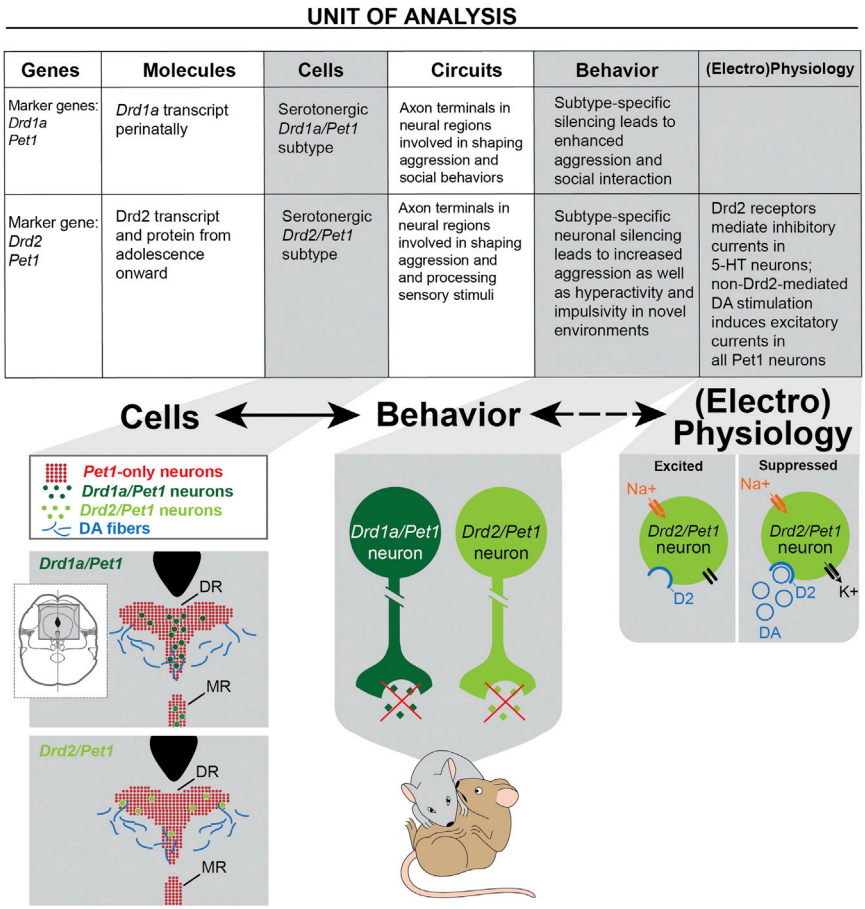

Figure 7. Summary of Findings within an RDoC-like Matrix

Chart summarizes findings within context of the NIMH RDoC matrix. Characteristics of the *Drd1a/Pet1* and *Drd2/Pet1* neuronal subtypes are subdivided among six of the RDoC "units of analysis" including *genes*, *molecules*, *cells*, *circuits* (*innervation*), *behavior*, and *(electro)physiology*. Schematics illustrate a subset of the key findings. From left to right: "Cells" illustrates the differential anatomical distribution of the *Drd/Pet1* subtypes and the *Pet1*-only 5-HT neurons in the DR. Dopaminergic fibers innervate the rostral DR (Kalén et al., 1988), where both *Drd/Pet1* and *Pet1*-only 5-HT neurons reside. "Behavior" shows that suppressed release of neurotransmitter (green diamonds) from either of the *Drd/Pet1* subtypes enhances aggression. "Electrophysiology" depicts the dopamine (blue circles)-induced inhibitory current (black arrow) mediated by D2 dopamine receptors (blue half circle) specifically in *Drd2/Pet1* neurons. The inhibitory current would counteract other excitatory currents (orange arrow) within the cell. Molecular genetic tools have facilitated relating "Cells" and "Behavior" findings (solid arrow), while it remains to be demonstrated that the Drd2-mediated inhibitory current in *Drd2/Pet1* 5-HT neurons influences aggressive behavior (dotted arrow).

Both the *Drd1a/Pet1* and the *Drd2/Pet1* subtypes send dense projections to the dopaminergic midbrain nuclei, namely the ventral tegmental area (VTA) and the substantia nigra pars compacta (SNc). Such a pattern suggests reciprocal circuitry, wherein midbrain dopaminergic neurons send projections to the rostral serotonergic system and vice versa (Niederkofler et al., 2015). Sources of dopaminergic innervation of the *Drd/Pet1* subtypes may include the rostral DR in addition to the SNc and midbrain VTA. Whereas the midbrain VTA dopaminergic neurons have been shown to directly impact aggressive behaviors (Yu et al., 2014), the rostral DR dopaminergic neurons have recently been shown to influence the subjective experience of social isolation (Matthews et al., 2016). It remains to be definitively demonstrated, however, whether dopamine-mediated regulation of serotonergic neurons influences serotonin-mediated modulation of aggressive behaviors.

Electrophysiology Suggests that Dopamine Differentially Influences *Drd2/Pet1* Neurons and *Pet1*-Only DR Serotonergic Neurons

Gene expression analysis and electrophysiology studies provide evidence for a direct effect of dopamine on subsets of serotonergic neurons that we have identified as shaping aggression. Transcriptional profiling of *Drd2/Pet1* neurons from adult animals confirmed the presence of *Drd2* transcript in nearly all cells analyzed, while electrophysiological studies further revealed that *Drd2/Pet1* neurons show a distinct functional response to dopamine as compared with *Pet1*-only neurons. Future studies will investigate the causal relationship between dopamine-induced inhibition of *Drd2/Pet1* neurons and aggression.

Multiscale Analysis of Inter-male Rodent Aggression

We investigated the neural correlates of aggression across multiple "units of analysis" as summarized in Figure 7 using a framework resembling the NIMH's RDoC (https://www.nimh.nih.gov/research-priorities/rdoc/constructs/rdoc-matrix.shtml). We identified two subtypes of serotonergic neurons ("cells"), each distinguished by the expression of either the *Drd1a* or *Drd2* marker genes along with serotonergic defining genes such as *Tph2*, *Pet1*, and *Slc6a4* (marker "genes"; Figure 7). We showed that silencing either of these neuronal subtypes enhanced aggressive behavior in adulthood ("behavior"). Further, we demonstrated that these serotonergic subtypes project to specific brain regions and reside in a region of the DR that receives dopaminergic innervation (the foundation for "circuitry" analyses). Our electrophysiological studies in turn demonstrate that, although dopamine has an excitatory effect on most serotonergic neurons, Drd2 expressed in the *Drd2/Pet1* neurons mediates an inhibitory current, which dampens the excitatory state of the cell ("physiology"). By considering neuronal subtypes underlying aggression at multiple biological levels, we are able to identify several points where further experimental investigation might: (1) elucidate substrates for

pharmacological treatments to temper impulsive aggression, and (2) further our understanding of how neuronal populations in the brain affect the generation and modulation of complex behaviors.

EXPERIMENTAL PROCEDURES

Detailed methods are provided in the Supplemental Experimental Procedures.

Mouse Lines

Procedures were in accord with institutional animal care and use committee policies at Harvard Medical School. Transgenics *Pet1::Flpe* (Jensen et al., 2008) and *ePet::cre* (Scott et al., 2005) were used to access serotonergic neurons. Transgenics *Drd1a::cre* (Gong et al., 2007), *Drd2::cre* (Gong et al., 2007), *Crf::cre* (https://www.mmrrc.org/catalog/sds.php?mmrrc_id=30850), and *(Rse2)HoxA2::cre* (Awatramani et al., 2003) and knockin transgene *Egr2::cre* (*Egr2*^{Cki}) (Voiculescu et al., 2000; Gong et al., 2007) targeted subsets of serotonergic cells when used intersectionally with *Pet1::Flpe*. Transgenics were backcrossed onto C57BL/6J for more than nine generations, with the exception of *Crf::cre*, which were a mixture of FVB/N, ICR, and C57BL/6 (https://www.mmrrc.org/catalog/sds.php?mmrrc_id=30850).

Recombinase lines were crossed to reporter or effector lines including *RC::FrePe* (Bang et al., 2012; Engleka et al., 2012) and its derivate *RC::rePe* (Cre-dependent only) (Ray et al., 2011), which encode a GFP reporter; *RC::PFtox* (Kim et al., 2009) and its derivate *RC::Ptox* (Cre-dependent only), which encode a tetanus toxin light chain-GFP fusion; and *RC::FPSit* encoding a synaptophysin-GFP fusion.

Resident-Intruder Assay

Species-typical aggression was studied using a resident-intruder (R-I) assay similar to previous reports (Miczek and O'Donnell, 1978; Fish et al., 1999). After weaning, transgenic male mice, "residents," were group-housed with male siblings until sexual maturity (~P55), when each resident was pair-housed with a female and sired pups. After 3.5–4 weeks, resident males were assayed for aggression toward a wild-type (CFW; Charles River) intruder mouse over the course of multiple trials until aggression stabilized, defined as the trial in which the average number of attack bites demonstrated by a single resident was within 20% variability of the previous three trials.

Behavioral Phenotyping

Except for R-I assays, all behavioral experiments were performed in the Harvard NeuroDiscovery Center following a two-week acclimation period, conducted in the order described in the Supplemental Experimental Procedures and involving mice 2–4.5 months of age at the beginning of the analysis.

Immunohistochemistry

Immunohistochemistry was used to assess localization and effectiveness of tetanus toxin light chain, anatomical distribution of targeted subsets of serotonin neurons, and projection patterns of targeted cell populations. Primary antibodies employed were chick anti-GFP (ab13970-100; Abcam) or rabbit anti-GFP (gift from Devreotes Lab), rabbit anti-dsRed to detect mCherry (632496; Clontech), goat anti-serotonin (ab66047; Abcam), and rabbit anti-Vamp2 (104202; Synaptic Systems).

Electrophysiology

Whole cell patch techniques were applied to fluorescently labeled neurons in mouse brain slices. Voltage clamp recordings were acquired from *Drd2*/*Pet1* (GFP$^+$) and *Pet1*-only (mCherry$^+$) neurons in the DR, and responses to dopamine (30 μM; Sigma), quinpirole (10–100 μM, D2-selective agonist; Sigma), or sulpiride (1 μM, D2-selective antagonist; Sigma) were measured. Current response to a voltage ramp from −100 to −30 mV over the course of ~1 min was used to extrapolate information about dopamine-induced currents. Details are provided in the Supplemental Experimental Procedures.

Gene Expression

Cell Sorting

Gene expression for select transcripts was assessed in a pooled sample (~30 cells) and single-cell samples for GFP$^+$ *Drd1a*/*Pet1* neurons, and single-cell samples from GFP$^+$ *Drd2*/*Pet1* and mCherry$^+$ (*Drd2*$^-$)/*Pet1* cells. As previously described (Hempel et al., 2007; Okaty et al., 2015), cells were isolated via protease treatment and physical dissociation by pipette trituration of DR brain tissue; individual neurons identified by fluorescent phenotype were collected by micropipette.

RNA Preparation

RNA was collected using a PicoPure RNA Isolation Kit (Arcturus), reverse transcribed to cDNA, and linearly amplified using the Ovation RNA-seq System V2 kit (Nugen).

RNA Sequencing

cDNA samples were sonicated (Covaris), integrated into RNA-seq libraries using the Ovation Ultralow DR Multiplex System 1-8 Kit (Nugen), quality controlled using TapeStation and qPCR, and sequenced using the Illumina HiSeq 2500 RNA-seq platform at the Harvard Biopolymers Facility.

Statistical Analyses

Behavior data were analyzed using statistical packages including Prism GraphPad, StatView 5.0 software (SAS Institute), Excel 2010, and Statistica (Dell). Statistical tests performed are given with relevant results with the exception of behavioral phenotyping data, which is included in Tables S4 and S5. Electrophysiology data were analyzed with Clampfit 9.2 software (Axon Instruments). Transcript sequence data were analyzed using edgeR (Anders et al., 2013; Okaty et al., 2015; Robinson et al., 2010).

ACCESSION NUMBERS

The accession number for the sequencing data reported in this paper is GEO: GSE87758.

SUPPLEMENTAL INFORMATION

Supplemental Information includes Supplemental Experimental Procedures, six figures, and seven tables and can be found with this article online at http://dx.doi.org/10.1016/j.celrep.2016.10.063.

AUTHOR CONTRIBUTIONS

V.N., T.E.A., and S.M.D. conceived the study. V.N. performed the behavioral experiments. V.N., T.E.A., and A.N. performed the histology and cell counts. V.N. and A.N. generated the *RC::FPSit* mouse. V.N. and T.E.A. quantified the projection targets. T.E.A. and B.W.O. performed the RT-PCR and RNA-seq experiments. B.D.R. performed the electrophysiological recordings, and S.G.B. consulted on electrophysiological experiments. L.S.H. performed the microdialysis and HPLC experiments. K.A.M. provided expertise in the resident-intruder paradigm. V.N., T.E.A., B.D.R., B.W.O., and S.M.D. wrote the manuscript.

ACKNOWLEDGMENTS

A portion of the behavioral work was carried out in the NeuroBehavior Laboratory Core subsidized by the Harvard NeuroDiscovery Center; we extend appreciation to Director Dr. Barbara Caldarone and S.M.D. laboratory members including Rebecca Senft for discussions and Drs. Rachael Brust and Ryan Dosumu-Johnson for pilot work. We thank Dr. Emily Newman, Mallory Rice, and Jia Jia Mai for technical assistance, and the HMS Biopolymers Facility Core for assistance in evaluating sample library quality and next-generation sequencing of samples. This work was supported by NIH grants AA021622 (L.S.H.), AA013983 (K.A.M.), 5R21DA023643-02 (V.N., T.E.A., A.N., and S.M.D.), R01 DA034022 (B.W.O., B.D.R., S.M.D., T.E.A., and V.N.), and R21MH083613 (S.M.D.). Additional support was provided by the G.V.R. Khodadad Program for the Study of Genetic, Neurobiological, and Physiochemical Processes of Excessive (Pathological) Selfishness and

Aggressive Behavior Fund at Harvard Medical School (V.N., B.W.O., and S.M.D.) and Swiss National Science Foundation grants PA00P3_131504 and PA00P3_142183 (V.N.).

Received: September 4, 2016
Revised: September 16, 2016
Accepted: October 17, 2016
Published: November 15, 2016

REFERENCES

Alenina, N., Kikic, D., Todiras, M., Mosienko, V., Qadri, F., Plehm, R., Boyé, P., Vilianovitch, L., Sohr, R., Tenner, K., et al. (2009). Growth retardation and altered autonomic control in mice lacking brain serotonin. Proc. Natl. Acad. Sci. USA *106*, 10332–10337.

Alonso, A., Merchán, P., Sandoval, J.E., Sánchez-Arrones, L., Garcia-Cazorla, A., Artuch, R., Ferrán, J.L., Martínez-de-la-Torre, M., and Puelles, L. (2013). Development of the serotonergic cells in murine raphe nuclei and their relations with rhombomeric domains. Brain Struct. Funct. *218*, 1229–1277.

American Psychiatric Association (2013). Diagnostic and Statistical Manual of Mental Disorders, Fifth Edition (American Psychiatric Association Publishing).

Anders, S., McCarthy, D.J., Chen, Y., Okoniewski, M., Smyth, G.K., Huber, W., and Robinson, M.D. (2013). Count-based differential expression analysis of RNA sequencing data using R and Bioconductor. Nat. Protoc. *8*, 1765–1786.

Angoa-Pérez, M., Kane, M.J., Briggs, D.I., Sykes, C.E., Shah, M.M., Francescutti, D.M., Rosenberg, D.R., Thomas, D.M., and Kuhn, D.M. (2012). Genetic depletion of brain 5HT reveals a common molecular pathway mediating compulsivity and impulsivity. J. Neurochem. *121*, 974–984.

Audero, E., Mlinar, B., Baccini, G., Skachokova, Z.K., Corradetti, R., and Gross, C. (2013). Suppression of serotonin neuron firing increases aggression in mice. J. Neurosci. *33*, 8678–8688.

Awatramani, R., Soriano, P., Rodriguez, C., Mai, J.J., and Dymecki, S.M. (2003). Cryptic boundaries in roof plate and choroid plexus identified by intersectional gene activation. Nat. Genet. *35*, 70–75.

Azmitia, E.C., and Segal, M. (1978). An autoradiographic analysis of the differential ascending projections of the dorsal and median raphe nuclei in the rat. J. Comp. Neurol. *179*, 641–667.

Bang, S.J., Jensen, P., Dymecki, S.M., and Commons, K.G. (2012). Projections and interconnections of genetically defined serotonin neurons in mice. Eur. J. Neurosci. *35*, 85–96.

Bond, A.J. (2005). Antidepressant treatments and human aggression. Eur. J. Pharmacol. *526*, 218–225.

Brust, R.D., Corcoran, A.E., Richerson, G.B., Nattie, E., and Dymecki, S.M. (2014). Functional and developmental identification of a molecular subtype of brain serotonergic neuron specialized to regulate breathing dynamics. Cell Rep. *9*, 2152–2165.

Coccaro, E.F., and Kavoussi, R.J. (1997). Fluoxetine and impulsive aggressive behavior in personality-disordered subjects. Arch. Gen. Psychiatry *54*, 1081–1088.

Commons, K.G., Connolley, K.R., and Valentino, R.J. (2003). A neurochemically distinct dorsal raphe-limbic circuit with a potential role in affective disorders. Neuropsychopharmacology *28*, 206–215.

Dahlstroem, A., and Fuxe, K. (1964). Evidence for the existence of monoamine-containing neurons in the central nervous system. I. Demonstration of monoamines in the cell bodies of brain stem neurons. Acta Physiol. Scand. Suppl. *232*, 1–55.

Dymecki, S.M., Ray, R.S., and Kim, J.C. (2010). Mapping cell fate and function using recombinase-based intersectional strategies. Methods Enzymol. *477*, 183–213.

Engleka, K.A., Manderfield, L.J., Brust, R.D., Li, L., Cohen, A., Dymecki, S.M., and Epstein, J.A. (2012). Islet1 derivatives in the heart are of both neural crest and second heart field origin. Circ. Res. *110*, 922–926.

Fernandez, S.P., Cauli, B., Cabezas, C., Muzerelle, A., Poncer, J.C., and Gaspar, P. (2015). Multiscale single-cell analysis reveals unique phenotypes of raphe 5-HT neurons projecting to the forebrain. Brain Struct. Funct. *221*, 4007–4025.

Fish, E.W., Faccidomo, S., and Miczek, K.A. (1999). Aggression heightened by alcohol or social instigation in mice: reduction by the 5-HT(1B) receptor agonist CP-94,253. Psychopharmacology (Berl.) *146*, 391–399.

Fox, S.R., and Deneris, E.S. (2012). Engrailed is required in maturing serotonin neurons to regulate the cytoarchitecture and survival of the dorsal raphe nucleus. J. Neurosci. *32*, 7832–7842.

Gaspar, P., and Lillesaar, C. (2012). Probing the diversity of serotonin neurons. Philos. Trans. R. Soc. Lond. B Biol. Sci. *367*, 2382–2394.

Gong, S., Doughty, M., Harbaugh, C.R., Cummins, A., Hatten, M.E., Heintz, N., and Gerfen, C.R. (2007). Targeting Cre recombinase to specific neuron populations with bacterial artificial chromosome constructs. J. Neurosci. *27*, 9817–9823.

Gross, C., Zhuang, X., Stark, K., Ramboz, S., Oosting, R., Kirby, L., Santarelli, L., Beck, S., and Hen, R. (2002). Serotonin1A receptor acts during development to establish normal anxiety-like behaviour in the adult. Nature *416*, 396–400.

Hale, M.W., and Lowry, C.A. (2011). Functional topography of midbrain and pontine serotonergic systems: implications for synaptic regulation of serotonergic circuits. Psychopharmacology (Berl.) *213*, 243–264.

Hale, M.W., Shekhar, A., and Lowry, C.A. (2012). Stress-related serotonergic systems: implications for symptomatology of anxiety and affective disorders. Cell. Mol. Neurobiol. *32*, 695–708.

Hempel, C.M., Sugino, K., and Nelson, S.B. (2007). A manual method for the purification of fluorescently labeled neurons from the mammalian brain. Nat. Protoc. *2*, 2924–2929.

Hendricks, T.J., Fyodorov, D.V., Wegman, L.J., Lelutiu, N.B., Pehek, E.A., Yamamoto, B., Silver, J., Weeber, E.J., Sweatt, J.D., and Deneris, E.S. (2003). Pet-1 ETS gene plays a critical role in 5-HT neuron development and is required for normal anxiety-like and aggressive behavior. Neuron *37*, 233–247.

Hollander, E. (1999). Managing aggressive behavior in patients with obsessive-compulsive disorder and borderline personality disorder. J. Clin. Psychiatry *60* (*Suppl 15*), 38–44.

Jensen, P., Farago, A.F., Awatramani, R.B., Scott, M.M., Deneris, E.S., and Dymecki, S.M. (2008). Redefining the serotonergic system by genetic lineage. Nat. Neurosci. *11*, 417–419.

Kähkönen, S., Yamashita, H., Rytsälä, H., Suominen, K., Ahveninen, J., and Isometsä, E. (2007). Dysfunction in early auditory processing in major depressive disorder revealed by combined MEG and EEG. J. Psychiatry Neurosci. *32*, 316–322.

Kalén, P., Skagerberg, G., and Lindvall, O. (1988). Projections from the ventral tegmental area and mesencephalic raphe to the dorsal raphe nucleus in the rat. Evidence for a minor dopaminergic component. Exp. Brain Res. *73*, 69–77.

Kim, J.C., Cook, M.N., Carey, M.R., Shen, C., Regehr, W.G., and Dymecki, S.M. (2009). Linking genetically defined neurons to behavior through a broadly applicable silencing allele. Neuron *63*, 305–315.

Lesage, F., Duprat, F., Fink, M., Guillemare, E., Coppola, T., Lazdunski, M., and Hugnot, J.P. (1994). Cloning provides evidence for a family of inward rectifier and G-protein coupled K+ channels in the brain. FEBS Lett. *353*, 37–42.

Lesch, K.P., and Merschdorf, U. (2000). Impulsivity, aggression, and serotonin: a molecular psychobiological perspective. Behav. Sci. Law *18*, 581–604.

Li, L., Tasic, B., Micheva, K.D., Ivanov, V.M., Spletter, M.L., Smith, S.J., and Luo, L. (2010). Visualizing the distribution of synapses from individual neurons in the mouse brain. PLoS ONE *5*, e11503.

Link, E., Edelmann, L., Chou, J.H., Binz, T., Yamasaki, S., Eisel, U., Baumert, M., Südhof, T.C., Niemann, H., and Jahn, R. (1992). Tetanus toxin action: inhibition of neurotransmitter release linked to synaptobrevin proteolysis. Biochem. Biophys. Res. Commun. *189*, 1017–1023.

Liu, C., Maejima, T., Wyler, S.C., Casadesus, G., Herlitze, S., and Deneris, E.S. (2010). Pet-1 is required across different stages of life to regulate serotonergic function. Nat. Neurosci. *13*, 1190–1198.

Lorenz, K. (1966). On Aggression (Methuen).

Lucker, J. R., and Doman, A. (2012). Auditory hypersensitivity and autism spectrum disorders: an emotional response. http://www.autismone.org/content/auditory-hypersensitivity-and-autism-spectrum-disorders-emotional-response-dr-jay-lucker-and.

Lucki, I. (1998). The spectrum of behaviors influenced by serotonin. Biol. Psychiatry *44*, 151–162.

Marler, P. (1976). On animal aggression. The roles of strangeness and familiarity. Am. Psychol. *31*, 239–246.

Matthews, G.A., Nieh, E.H., Vander Weele, C.M., Halbert, S.A., Pradhan, R.V., Yosafat, A.S., Glober, G.F., Izadmehr, E.M., Thomas, R.E., Lacy, G.D., et al. (2016). Dorsal raphe dopamine neurons represent the experience of social isolation. Cell *164*, 617–631.

Miczek, K.A., and O'Donnell, J.M. (1978). Intruder-evoked aggression in isolated and nonisolated mice: effects of psychomotor stimulants and L-dopa. Psychopharmacology (Berl.) *57*, 47–55.

Molliver, M.E. (1987). Serotonergic neuronal systems: what their anatomic organization tells us about function. J. Clin. Psychopharmacol. *7* (*6 Suppl*), 3S–23S.

Mosienko, V., Bert, B., Beis, D., Matthes, S., Fink, H., Bader, M., and Alenina, N. (2012). Exaggerated aggression and decreased anxiety in mice deficient in brain serotonin. Transl. Psychiatry *2*, e122.

Nelson, R.J., and Trainor, B.C. (2007). Neural mechanisms of aggression. Nat. Rev. Neurosci. *8*, 536–546.

Niederkofler, V., Asher, T.E., and Dymecki, S.M. (2015). Functional interplay between dopaminergic and serotonergic neuronal systems during development and adulthood. ACS Chem. Neurosci. *6*, 1055–1070.

Okaty, B.W., Freret, M.E., Rood, B.D., Brust, R.D., Hennessy, M.L., deBairos, D., Kim, J.C., Cook, M.N., and Dymecki, S.M. (2015). Multi-scale molecular deconstruction of the serotonin neuron system. Neuron *88*, 774–791.

Peyron, C., Luppi, P.H., Kitahama, K., Fort, P., Hermann, D.M., and Jouvet, M. (1995). Origin of the dopaminergic innervation of the rat dorsal raphe nucleus. Neuroreport *6*, 2527–2531.

Ray, R.S., Corcoran, A.E., Brust, R.D., Kim, J.C., Richerson, G.B., Nattie, E., and Dymecki, S.M. (2011). Impaired respiratory and body temperature control upon acute serotonergic neuron inhibition. Science *333*, 637–642.

Reist, C., Nakamura, K., Sagart, E., Sokolski, K.N., and Fujimoto, K.A. (2003). Impulsive aggressive behavior: open-label treatment with citalopram. J. Clin. Psychiatry *64*, 81–85.

Robinson, M.D., McCarthy, D.J., and Smyth, G.K. (2010). edgeR: a Bioconductor package for differential expression analysis of digital gene expression data. Bioinformatics *26*, 139–140.

Rood, B.D., Calizo, L.H., Piel, D., Spangler, Z.P., Campbell, K., and Beck, S.G. (2014). Dorsal raphe serotonin neurons in mice: immature hyperexcitability transitions to adult state during first three postnatal weeks suggesting sensitive period for environmental perturbation. J. Neurosci. *34*, 4809–4821.

Rothman, R.B., Clark, R.D., Partilla, J.S., and Baumann, M.H. (2003). (+)-Fenfluramine and its major metabolite, (+)-norfenfluramine, are potent substrates for norepinephrine transporters. J. Pharmacol. Exp. Ther. *305*, 1191–1199.

Sahlholm, K., Marcellino, D., Nilsson, J., Fuxe, K., and Arhem, P. (2008). Differential voltage-sensitivity of D2-like dopamine receptors. Biochem. Biophys. Res. Commun. *374*, 496–501.

Saudou, F., Amara, D.A., Dierich, A., LeMeur, M., Ramboz, S., Segu, L., Buhot, M.C., and Hen, R. (1994). Enhanced aggressive behavior in mice lacking 5-HT1B receptor. Science *265*, 1875–1878.

Scott, M.M., Wylie, C.J., Lerch, J.K., Murphy, R., Lobur, K., Herlitze, S., Jiang, W., Conlon, R.A., Strowbridge, B.W., and Deneris, E.S. (2005). A genetic approach to access serotonin neurons for in vivo and in vitro studies. Proc. Natl. Acad. Sci. USA *102*, 16472–16477.

Spaethling, J.M., Piel, D., Dueck, H., Buckley, P.T., Morris, J.F., Fisher, S.A., Lee, J., Sul, J.Y., Kim, J., Bartfai, T., et al. (2014). Serotonergic neuron regulation informed by in vivo single-cell transcriptomics. FASEB J. *28*, 771–780.

Steinbusch, H.W. (1981). Distribution of serotonin-immunoreactivity in the central nervous system of the rat-cell bodies and terminals. Neuroscience *6*, 557–618.

Takahashi, A., and Miczek, K.A. (2014). Neurogenetics of aggressive behavior: studies in rodents. Curr. Top. Behav. Neurosci. *17*, 3–44.

Voiculescu, O., Charnay, P., and Schneider-Maunoury, S. (2000). Expression pattern of a Krox-20/Cre knock-in allele in the developing hindbrain, bones, and peripheral nervous system. Genesis *26*, 123–126.

Volavka, J. (2002). Neurobiology of Violence (American Psychiatric Association Publishing).

Wylie, C.J., Hendricks, T.J., Zhang, B., Wang, L., Lu, P., Leahy, P., Fox, S., Maeno, H., and Deneris, E.S. (2010). Distinct transcriptomes define rostral and caudal serotonin neurons. J. Neurosci. *30*, 670–684.

Wyss, C., Hitz, K., Hengartner, M.P., Theodoridou, A., Obermann, C., Uhl, I., Roser, P., Grünblatt, E., Seifritz, E., Juckel, G., and Kawohl, W. (2013). The loudness dependence of auditory evoked potentials (LDAEP) as an indicator of serotonergic dysfunction in patients with predominant schizophrenic negative symptoms. PLoS ONE *8*, e68650.

Yu, Q., Teixeira, C.M., Mahadevia, D., Huang, Y., Balsam, D., Mann, J.J., Gingrich, J.A., and Ansorge, M.S. (2014). Dopamine and serotonin signaling during two sensitive developmental periods differentially impact adult aggressive and affective behaviors in mice. Mol. Psychiatry *19*, 688–698.

Zalsman, G., Patya, M., Frisch, A., Ofek, H., Schapir, L., Blum, I., Harell, D., Apter, A., Weizman, A., and Tyano, S. (2011). Association of polymorphisms of the serotonergic pathways with clinical traits of impulsive-aggression and suicidality in adolescents: a multi-center study. World J. Biol. Psychiatry *12*, 33–41.